Received: 12 June 2023 | Revised: 29 January 2024 | Accepted: 1 February 2024

DOI: 10.1002/ardp.202300319

ARCH PHARM DPhG
Archiv der Pharmazie

FULL PAPER

Novel quinoline derivatives with broad-spectrum antiprotozoal activities

Carla B. Hartman[1] | Phelelisiwe S. Dube[1] | Lesetja J. Legoabe[1] | Natascha Van Pelt[2] | An Matheeussen[2] | Guy Caljon[2] | Richard M. Beteck[1]

[1]Centre of Excellence for Pharmaceutical Sciences, North-West University, Potchefstroom, South Africa

[2]Laboratory of Microbiology, Parasitology and Hygiene, Infla-Med Centre of Excellence, University of Antwerp, Antwerp, Belgium

Correspondence
Richard M. Beteck, Centre of Excellence for Pharmaceutical Sciences, North-West University, Private Bag X6001, Potchefstroom 2520, South Africa.
Email: 25159194@nwu.ac.za and richmbi1@yahoo.com

Guy Caljon, Laboratory of Microbiology, Parasitology and Hygiene, Infla-Med Centre of Excellence, University of Antwerp, Antwerp 2610, Belgium.
Email: Guy.Caljon@uantwerpen.be

Funding information
South African Medical Research Council

Abstract

Several quinoline derivatives incorporating arylnitro and aminochalcone moieties were synthesized and evaluated in vitro against a broad panel of trypanosomatid protozoan parasites responsible for sleeping sickness (*Trypanosoma brucei rhodesiense*), nagana (*Trypanosoma brucei brucei*), Chagas disease (*Trypanosoma cruzi*), and leishmaniasis (*Leishmania infantum*). Several of the compounds demonstrated significant antiprotozoal activity. Specifically, compounds **2c**, **2d**, and **4i** displayed submicromolar activity against *T. b. rhodesiense* with half-maximal effective concentration (EC_{50}) values of 0.68, 0.8, and 0.19 µM, respectively, and with a high selectivity relative to human lung fibroblasts and mouse primary macrophages (~100-fold). Compounds **2d** and **4i** also showed considerable activity against *T. b. brucei* with EC_{50} values of 1.4 and 0.4 µM, respectively.

KEYWORDS
anti-infectives, arylnitro, chalcones, protozoal, quinoline

1 | INTRODUCTION

Trypanosomatids are responsible for a range of neglected parasitic diseases, including human African trypanosomiasis (HAT) and animal African trypanosomiasis (AAT), Chagas disease, and leishmaniasis.[1] *Trypanosoma brucei gambiense* and *Trypanosoma brucei rhodesiense* are responsible for HAT, commonly referred to as sleeping sickness.[2] HAT occurs in sub-Saharan Africa and its prevalence is largely influenced by the presence of the *tsetse* fly vector and the implementation of control measures. Unfortunately, during political unrest, control measures tend to be disregarded, leading to the re-emergence of the disease.[3] *T. b. gambiense* accounts for 98% of HAT cases and is primarily found in West and Central Africa, while *T. b. rhodesiense* causes 2% of HAT cases and it is mainly prevalent in East and Southern Africa.[4] *T. b. rhodesiense* infections are more severe, leading to acute infections and potential death within a few months of initiation. *T. b. gambiense*, on the other hand, causes chronic infections lasting several years.[5] Symptoms for both species vary according to the disease stage, with the first stage exhibiting intermittent fever, headache, pruritus, endocrine dysfunction, lymphadenopathy, edema, and hepatosplenomegaly.[6] During the second stage, when the parasites infiltrate the central nervous system, patients may experience neuropsychiatric disorders such as sleep disturbances, tremors of the fingers and hands, motor weakness, speech disorders, attention deficit, confusion, and emotional lability.[6] If left untreated, this disease can be fatal, particularly if the parasites have already crossed the blood-brain barrier.[7]

AAT, commonly referred to as nagana, is a parasitic disease affecting livestock in sub-Saharan Africa.[8] The causative agents of this disease are *Trypanosoma congolense*, *Trypanosoma vivax*, and

Trypanosoma brucei brucei.[9] Infection results in debilitating symptoms, including anemia and cachexia, that may eventually result in death. Livestock productivity is severely hindered by nagana, which consequently poses a serious risk to food security and economic growth in sub-Saharan Africa.[10]

Trypanosoma cruzi, transmitted by kissing bugs and other horizontal and vertical routes (blood transfusion, contaminated food and drinks, congenital transmission), causes Chagas disease, mainly prevalent in Latin America.[11] This vector-borne illness affects millions of people and can remain asymptomatic over a prolonged period of time, eventually resulting in a chronic disease with severe cardiac and gastrointestinal complications.[12]

Leishmaniasis is a family of related parasitic diseases caused by hemoflagellate *Leishmania* spp. that is transmitted to humans primarily through the bites of infected female phlebotomine sand flies.[13] Clinical manifestations vary from a cutaneous to a destructive and stigmatizing mucocutaneous to a lethal visceral form of the disease (kala-azar) and post-kala-azar dermal leishmaniasis.[13] Leishmaniasis is endemic in at least 88 countries located in different regions of the world and disproportionately affects the poorest populations.[14]

Although there have been promising developments for these trypanosomatids diseases,[15] several challenges remain, and many of the available treatment options (Figure 1) are plagued by issues such as the need for parenteral administration over prolonged periods of time, toxicity, or resistance affecting efficacy and the patient's compliance to the treatment regimens. These limitations necessitate the development of newer and more effective therapeutic interventions.[13]

Quinoline is an extensively studied class of heterocyclic compounds.[16] Quinoline derivatives are widely distributed in nature and have garnered great interest in medicinal chemistry due to their ability to serve as versatile scaffolds for the development of compounds with diverse biological activities.[17] Numerous quinoline derivatives have shown efficacy in vitro against the causal agents of neglected diseases such as *T. brucei*[18,19] leishmania parasites,[20] as well as other infectious agents, including *Mycobacterium tuberculosis*,[21] certain ESKAPE pathogens.[22] Like quinolines, chalcones exhibit a wide range of biological activities, including antiplasmodial,[23,24] antiviral,[25] antiprotozoal,[26] and anticancer activities.[27] Among the various chalcone derivatives, aminochalcones have potential as antileishmanial,[28] antitrypanosomal,[29] and antibacterial agents.[30]

Nitroaromatic chemicals have been found to exhibit inhibitory effects against various pathogenic organisms, including bacteria,[31,32] fungi,[33] viruses, and protozoans.[34] Typically, they function as prodrugs, wherein the nitro group is bioreduced to generate reactive nitrogen species, which are responsible for the anti-infective properties of this compound class.[35] The pharmacological properties of nitroaromatic compounds are influenced by several factors, such as the size of the aryl ring (five- or six-membered) to which the nitro moiety is attached, the presence of heteroatoms (N, S, O) in the ring, and electronic properties of substituents appended to the aryl ring.[34]

In this study, we conceptualized a designed strategy to hybridize the quinolinyl, aminochalconyl, and arylnitro moieties into a single molecule (Figure 2) with the hope of identifying broad-spectrum antiprotozoal agents. The compounds were screened against several parasitic protozoans, and they generally showed broad-spectrum antiprotozoal activities.

2 | RESULTS AND DISCUSSION

2.1 | Chemistry and structure characterization

The synthesis of target compounds was achieved using synthetic procedures depicted in Scheme 1. The starting material, 4,7-dichloroquinoline, was subjected to nucleophilic substitution reaction with appropriate anilines[36] to generate intermediates **1** and **2**. Intermediate **1** was then subjected to a Schiff base condensation reaction[37] with 5-nitrofuran-2-carbaldehyde to yield compound **1a** with a yield of 59%. Intermediate **2** was subjected to an Aldol condensation reaction[32] with various aldehydes, affording compounds **2a–2d** in yields ranging from 30% to 100%. To synthesize compounds **3a–3d**, intermediate **2** underwent *N*-alkylation with appropriate benzyl halide.[36] This reaction afforded the desired compounds with yields varying from 10% to 80%. In addition, compounds **3a–3d** were subjected to Aldol condensation[32]

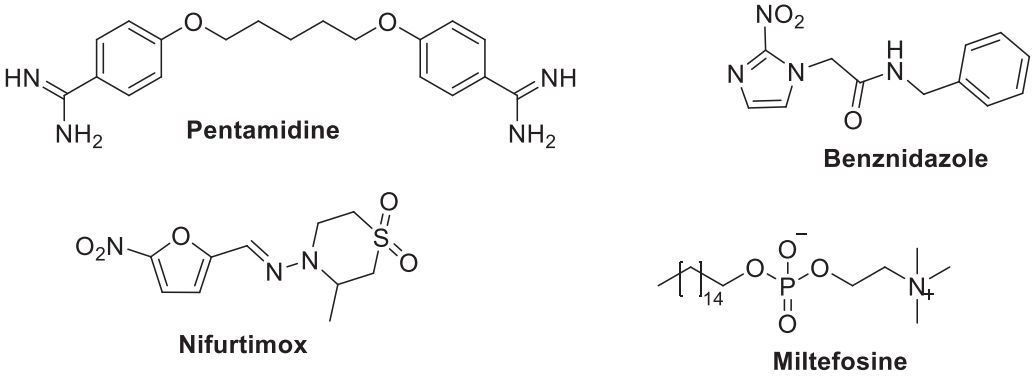

FIGURE 1 Drugs used to treat trypanosomatids diseases.

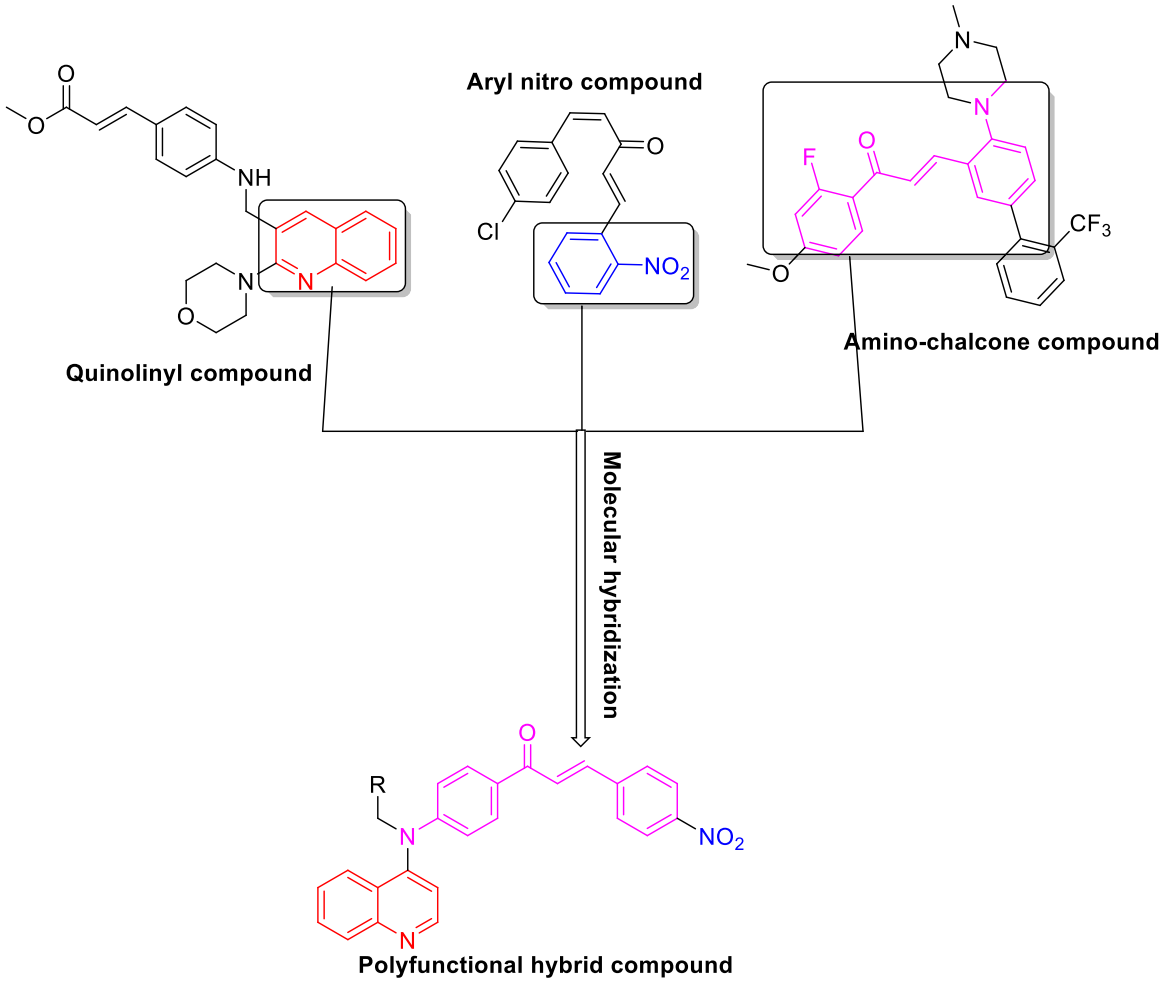

FIGURE 2 Structural design of target compounds.

with various aldehydes in acetic acid, resulting in the formation of compounds **4a–4i** with yields ranging from 5% to 50%.

Proton and carbon-13 nuclear magnetic resonance (NMR) were used to characterize all target compounds. The appearance or absence/disappearance of certain peaks was used to confirm successful synthetic transformation(s). The absence of a singlet peak at around 5 ppm (attributable to the –NH2 moiety of **1**) on the proton NMR of compound **1a** implies that the Schiff base condensation was successful. The absence of the peaks at around 2.4 and 30 ppm (attributable to the $-CH_3$ moiety of **2** and **3a–3d**) in the ^1H and ^{13}C, respectively, of compounds **2a–2d** and **4a–4i** indicate that the aldol condensation reaction was successful. Moreover, all aldol condensation products contain doublet in the ^1H NMR at approximately 7.2 ppm, which is assignable to protons within the alkenyl unit conjugated to ketone. The peak ca. 187 ppm on ^{13}C NMR is attributed to the ketone carbon (C=O). For compounds **4a–4i**, the N-methylenyl (N-CH_2–) unit appears ca. 5.6 and 56 ppm on the ^1H and ^{13}C NMR spectra, respectively. Several of the target compounds also include small amounts of solvent impurities in their NMR spectra, such as ethanol. The target compounds were vacuum-dried for 72 h to get rid of solvent contaminants before biological testing. High-resolution mass spectra (HRMS) were used to verify the molecular mass of each compound.

2.2 | Antiprotozoal activity

Compounds in this study were evaluated for antiprotozoal activities against the causal agents of Chagas disease, leishmaniasis, HAT, and nagana. Benznidazole, miltefosine, and suramin were included as reference drugs. The compounds were also evaluated for overt toxicity using MRC-5 human fibroblasts and primary mouse macrophages. Tamoxifen was included as a reference in the toxicity assays.

T. brucei Squib 427 and *T. b. rhodesiense* STIB-90050 were cultured at a density of 1.5×10^4 and 4×10^3 parasites per well, respectively. For *Leishmania infantum* and *T. cruzi*, host cells were infected with 4.5×10^5 and 4×10^4 parasites per well, respectively, and cultured. The cultured parasites were incubated with test samples at varying concentrations, after which parasite viability at these different concentrations was assessed either spectrophotometrically (*T. cruzi*, *T. brucei*, and *T. b. rhodesiense*) or microscopically (*L. infantum*). Percentage parasite viability was recorded against the

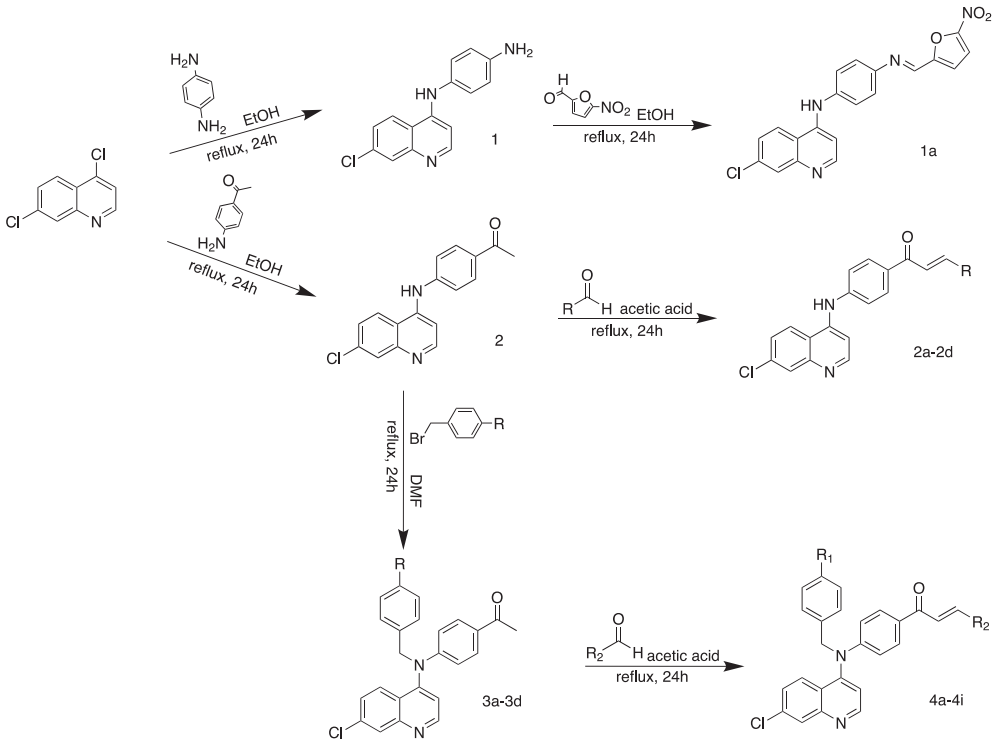

*percentage yield

R

2a: 92%*, 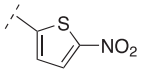

2b: 88%*, 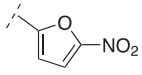

2c: 32%*, 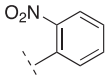

2d: 62%*, 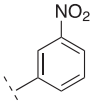

3a: 71%*, CH_3

3b: 32%*, H

3c: 18%*, Br

3d: 39%*, CF_3

4a: 45%*, R_1: CH_3, R_2: 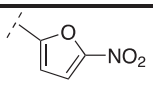

4b: 8%*, R_1: CH_3, R_2: 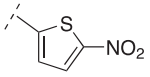

4c: 14%*, R_1: CH_3, R_2: 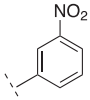

4d: 26%*, R_1: CH_3, R_2: 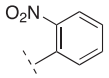

4e: 27%*, R_1: H, R_2: 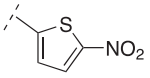

4f: 22%*, R_1: Br, R_2: 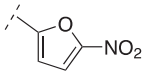

4g: 35%*, R_1: CF_3, R_2: 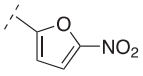

4h: 21%*, R_1: CF_3, R_2: 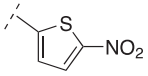

4i: 20%*, R_1: CF_3, R_2: 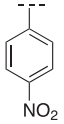

SCHEME 1 Synthesis of the target compounds.

corresponding compound concentration, and these data were used to generate the half-maximal effective concentration (EC_{50}) values.

As indicated in Table 1, most of the compounds in this study demonstrated potent and broad-spectrum antiprotozoal activities. However, several of these compounds also exhibited severe cytotoxicity towards both MRC-5 human fibroblasts and primary mouse macrophages. Among the active compounds, notably **2c**, **2d**, and **4i** demonstrated potent antiprotozoal activity while exhibiting little to no cytotoxicity with selectivity indices approaching or surpassing 100 for the African trypanosome species.

Compounds **2c** and **2d** demonstrated submicromolar EC_{50} values against the causal agents of nagana and HAT. Compound **2c** had an EC_{50} value of 0.68 μM against *T. b. rhodesiense*, while compound **2d** showed EC_{50} values of 1.4 and 0.8 μM against *T. b. brucei* and *T. b. rhodesiense*, respectively. Both of these compounds contain a nitro (NO_2) functional group, with the only difference being the position of the nitro moiety. Compound **2d**, which has the nitro group at the third position, showed higher activity against both *T. b. brucei* and *T. b. rhodesiense* compared to **2c**, which has the nitro group at the second position. This suggests that the position of the nitro group on the aromatic ring plays a critical role in determining the potency of the compounds against these protozoan parasites.

Compound **3d** exhibited some antileishmanial activity, with an EC_{50} value of 8.83 μM against *L. infantum*. This in vitro activity profile is comparable to that exhibited by the antileishmanial drug miltefosine (IC_{50}: 6.35 μM).

Compound **4i** has potent EC_{50} values of 0.43 μM against *T. b. brucei*, 0.19 μM against *T. b. rhodesiense*, 4.6 μM against *T. cruzi*, and 10.1 μM against *L. infantum*. The activity profile of this compound against *T. cruzi*, and *L. infantum* is comparable to that recorded for the reference drugs. Compound **4i** does have broad spectrum antiprotozoal activities and is not toxic to primary mouse microphages and MRC-5 cells at the concentration required to achieve antiprotozoal activities.

Generally, it could be observed that compounds containing six-membered arylnitro (**2c–2d**, **4c–4d**, **4i**) possessed better intrinsic antiprotozoal activities than their corresponding analogs bearing five-membered arylnitro unit (**2a–2b**, **4e–4h**). For example, compound **2c** has more than twofold better activity than **2a** against all protozoal strains deployed, except against *T. cruzi* wherein **2a** (EC_{50}: 8.12 μM) shows superior activity against **2c** (EC_{50}: 32 μM). Compound **4i** shows better activity over **4h** against *T. b. brucei* and *T. b. rhodesiense*, while **4h** (EC_{50}: 0.46 μM) maintained lower EC_{50} values than **4i** (EC_{50}: 4 μM) against *T. cuzi*.

Moreover, the nature of the amine also influenced antiprotozoal activities and toxicity. Converting the secondary amine at position 4 of the quinoline ring to a tertiary amine increases antiprotozoal activities, as well as cell toxicity. For example, compound **2d** showed higher EC_{50} values against all the targets than its tertiary amine derivative, **4c**. Derivatizing **2a** to **4b** led to an over 10-fold increase in antiprotozoal activities as well as toxicity against MRC-5 cells. Derivative **4b** has submicromolar activities against trypanosome parasites and moderate activity (EC_{50}: 10 μM) against *L. infantum*. Two tertiary amine derivatives, compounds **3d** and **4i**, were, however, not toxic to MRC-5 and primary mouse macrophages.

With regard to compounds containing five-membered arylnitro unit, nitrofuranyl-bearing compounds generally showed better antiprotozoal activities than their nitrothiopnenyl analogs. The activity difference against trypanosomes (*T. cruzi*, *T. b. brucei*, and *T. b. rhodesiense*) in most cases is not very significant. This difference is often greater than twofold against *L. infantum*. For example, compound **4a** (EC_{50}: 1.5 μM) is six times more active against *L. infantum* than its nitrothiopnenyl analog, **4b** (EC_{50}: 10 μM). This trend follows suit with the following pairs of analogs: **4g** (EC_{50}: 0.6 μM) versus **4h** (EC_{50}: 1.5 μM), **2b** (EC_{50}: 26.5 μM) versus **2a** (EC_{50}: 36.7 μM). Moreover, it could be observed that the nitrothiopnenyl-bearing compounds show lower cell toxicity potential than nitrofuranyl-bearing compounds. For example, compound **2a** is nontoxic to MRC-5 (EC_{50}: >64 μM), while compound **2b** showed low micromolar activity of 5 μM against MRC-5. This is also observed in compounds **4g** (EC_{50}: 0.23 μM) against **4h** (EC_{50}: 1.3 μM). Nitrothiopnenyl-bearing compounds generally had less toxicity against PMM than their nitrofuranyl analogs. Compound **4b** (EC_{50}: >64 μM) had no activity on PMM, while its nitrofuranyl analog **4a** recorded higher activity (EC_{50}: 32 μM). This trend is observed in **4h** (EC_{50}: 32 μM) against **4g** (EC_{50}: 8 μM).

3 | CONCLUSION

In this project, we have successfully synthesized novel 4,7-disubstituted quinoline derivatives. The compounds were subjected to in vitro evaluation to determine their antiprotozoal activities. Notably, numerous compounds demonstrated significant and selective antiprotozoal activity with IC_{50} values of less than 5 μM. Compounds **2c**, **2d**, and **4i** displayed notable activity against *T. b. rhodesiense* with IC_{50} values of 0.68, 0.8, and 0.19 μM, respectively. Compounds **2d** and **4i** also showed potent activity against *T. b. brucei*, with IC_{50} values of 1.4 and 0.4 μM, respectively. Compounds **3d** and **4i** exhibited antileishmanial activity with IC_{50} values of 8.83 and 10 μM, respectively.

4 | EXPERIMENTAL

4.1 | Chemistry

4.1.1 | General

Reagents and solvents were purchased from chemical vendors such as Sigma-Aldrich, Ace, Rochelle, Ambeed, and were utilized as supplied. Merck $60F_{254}$ silica gel plates supported by 0.20 mm thick aluminum sheets were used to track reaction progression. Samples were dissolved in deuterated DMSO-d_6, and a Bruker Advance III 600 spectrophotometer was used to record their ^1H and ^{13}C NMR spectra at 600 and 151 MHz, respectively. MestResNova version 10

TABLE 1 Structures, antiprotozoal activities, and cytotoxicity of compounds **2a–2d**, **3d**, and **4a–4i**.

ID	Structure	MRC-5 CC_{50} (μM)[a]	*Trypanosoma cruzi* EC_{50} (μM)[a]	*Leishmania infantum* EC_{50} (μM)[a]	*Trypanosoma brucei* EC_{50} (μM)[a]	*Trypanosoma brucei rhodesiense* EC_{50} (μM)[a]	PMM CC_{50} (μM)[a]
2a	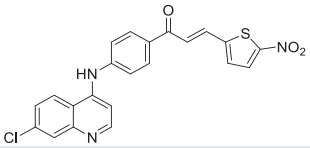	>64	8.12	36.76	8.90	7.21	>64
2b	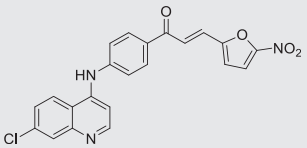	5.22	1.95	26.49	1.93	1.93	>64
2c	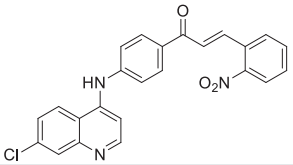	>64	32.90	12.70	2.52	0.68	>64
2d[38]	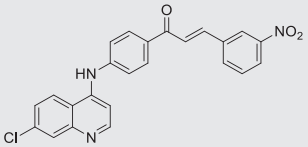	>64	20.4 ± 8.3	40 ± 17.3	1.4 ± 0.89	0.8 ± 0.24	>64
3d	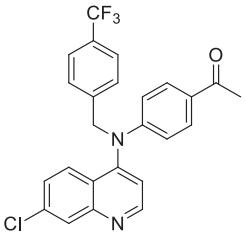	>64	>64	8.83	>64	>64	>64
4a	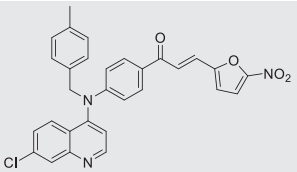	1.41	0.52	1.59	0.46	0.5	32
4b	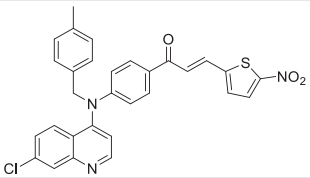	0.94	0.20	10.08	0.40	0.13	>64
4c	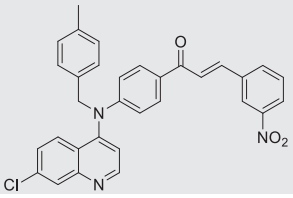	6.62	1.69	0.50	0.21	0.42	8
4d	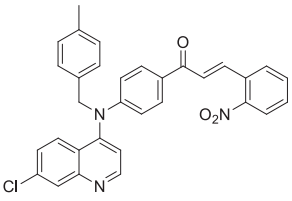	6.96	2.00	1.39	0.32	0.47	2

TABLE 1 (Continued)

ID	Structure	MRC-5 CC_{50} (μM)[a]	*Trypanosoma cruzi* EC_{50} (μM)[a]	*Leishmania infantum* EC_{50} (μM)[a]	*Trypanosoma brucei* EC_{50} (μM)[a]	*Trypanosoma brucei rhodesiense* EC_{50} (μM)[a]	PMM CC_{50} (μM)[a]
4e	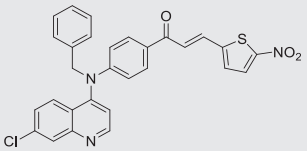	2.36	0.37	2.16	0.47	0.50	>64
4f	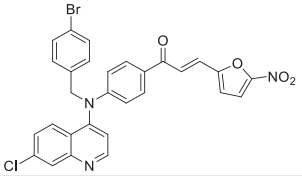	1.15	0.53	1.78	0.50	0.49	8
4g	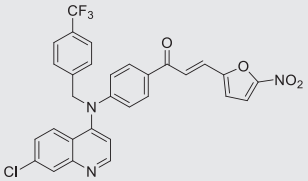	0.23	0.13	0.63	0.11	0.13	8
4h	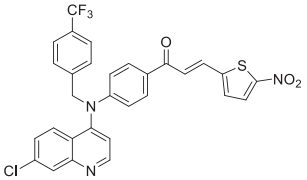	1.31	0.46	1.49	0.47	0.50	32
4i	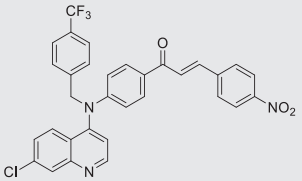	39 ± 2.2	4.6 ± 3.4	10.1 ± 2.9	0.43 ± 0.15	0.19 ± 2.8	>64
TF		10.27					
BZN			1.47				
MF				6.35			
SUR					0.05	0.04	

Note: Reference drugs: tamoxifen (TF), benznidazole (BZN), miltefosine (MF), and suramin (SUR).

Abbreviation: PMM, primary mouse microphage.

[a]Inhibitory concentration.

was used for the analysis of NMR data. Chemical shifts are given in parts per million (ppm) and were compared to solvent peaks (DMSO-d_6: 2.50 and 39.52 ppm for ^{1}H and ^{13}C NMR, respectively; see the Supporting Information). Spin multiplicities are denoted by the letters s for singlet, d for doublet, t for triplets, m for multiplet, dt for doublet of triplets, td for triplet of doublets, and dd for doublet of doublets. Coupling constants (*J*) are given in Hz. HRMS were captured using a Bruker micrOTOF-Q II mass spectrometer in positive ion mode using atmospheric pressure chemical ionization (APCI). With a capillary voltage of 4500 V, an end plate offset of −500 V, 1.8 bar nebulizers, and a collision cell RF voltage of 150 V_{pp}, a complete scan from 50 to 1600 *m/z* was performed. A Bruker ALPHA FTIR Routine spectrometer was used to perform Fourier-transform infrared spectroscopy (FTIR).

The InChI codes of the investigated compounds, together with some biological activity data, are provided as Supporting Information.

4.1.2 | Synthesis of compound **1a**

In a round bottom flask equipped with a reflux condenser, 1.0 g (5 mmol) of 4,7-dichloroquinoline was heated under reflux for 24 h with 1.2 equivalents (6.1 mmol) of *p*-phenylenediamine in 20 mL of ethanol as the solvent. The reaction progression was monitored by thin-layer chromatography (TLC). After completion of the reaction, the reaction mixture was allowed to cool to room temperature, and the formed solid precipitate was filtered. The resulting solid was dried to yield intermediate **1**.

Next, 0.5 g (1.9 mmol) of intermediate **1** was added to a round bottom flask with 1.5 equivalents (2.8 mmol) of 5-nitro-2-furaldehyde. The reaction was carried out in 15 mL of ethanol with 0.5 mL of acetic acid as the catalyst. The mixture was refluxed for 24 h and monitored using TLC. Upon completion of the reaction, excess aldehyde was removed by hot filtration. The solid residue was dried to afford compound **1a**.

(*E*)-7-Chloro-*N*-{4-[(5-nitrofuran-2-yl)methyleneamino]phenyl} quinolin-4-amine (**1a**). Orange powder; 59% yield; m.p.: 238–240°C; ^{1}H NMR (600 MHz, DMSO-d$_6$) δ 8.91 (d, *J* = 9.1 Hz, 1H), 8.73 (s, 1H), 8.56 (d, *J* = 6.9 Hz, 1H), 8.19 (d, *J* = 2.1 Hz, 1H), 7.90–7.81 (m, 2H), 7.59–7.40 (m, 4H), 7.49 (d, *J* = 3.9 Hz, 1H), 6.91 (d, *J* = 6.9 Hz, 1H). ^{13}C NMR (151 MHz, DMSO-d$_6$) δ 154.81, 153.15, 152.92, 148.89, 148.78, 144.31, 140.03, 138.71, 136.92, 127.78, 127.01, 126.66, 126.46, 123.45, 120.08, 118.88, 116.70, 114.66, 101.14. HRMS-APCI *m/z* calcd for $C_{20}H_{14}ClN_4O_3$ $[M+H]^+$, 393.0768, found 393.0749.

4.1.3 | Synthesis of compounds **2a–2d** and **4a–4i**

A round bottom flask was charged with 0.3 g (1 mmol) of intermediate **2**, 1.5 equivalents of appropriate aldehydes, and 10–15 mL of acetic acid as a solvent, along with catalytic amounts of sulfuric acid. The reaction was refluxed for 24 h and monitored with TLC. After completion, the reaction was cooled to room temperature and added to ice, then stirred for approximately 1 h. It was then filtered and washed with water to afford target compounds **2a–2d**. This same procedure was used to generate compounds **4a–4d**, starting with intermediate **3a–3d**.

(*E*)-1-{4-[(7-Chloroquinolin-4-yl)amino]phenyl}-3-(5-nitrothiophen-2-yl)prop-2-en-1-one (**2a**). Green powder; 92% yield; m.p.: 189–191°C; ^{1}H NMR (600 MHz, DMSO-d$_6$) δ 8.66 (d, *J* = 5.9 Hz, 1H), 8.55 (d, *J* = 9.1 Hz, 1H), 8.28 (d, *J* = 8.5 Hz, 2H), 8.18 (d, *J* = 4.3 Hz, 1H), 8.05–8.00 (m, 2H), 7.91 (d, *J* = 15.5 Hz, 1H), 7.80 (dd, *J* = 15.1, 6.9 Hz, 2H), 7.59 (d, *J* = 8.5 Hz, 2H), 7.26 (d, *J* = 6.0 Hz, 1H). ^{13}C NMR (151 MHz, DMSO-d$_6$) δ 187.22, 164.63, 159.03, 152.06, 150.13, 147.26, 145.25, 136.79, 134.87, 133.30, 131.43, 131.20, 131.06, 127.14, 126.11, 125.75, 124.57, 121.93, 118.67, 104.36. HRMS-APCI *m/z* calcd for $C_{22}H_{15}ClN_3O_3S$ $[M+H]^+$, 436.0524, found 436.0517.

(*E*)-1-{4-[(7-Chloroquinolin-4-yl)amino]phenyl}-3-(5-nitrofuran-2-yl)prop-2-en-1-one (**2b**). Brown powder; 88% yield; m.p.: 258–260°C; ^{1}H NMR (600 MHz, DMSO-d$_6$) δ 8.65 (d, *J* = 5.9 Hz, 1H), 8.56 (dd, *J* = 9.3, 9.1 Hz, 1H), 8.22 (d, *J* = 8.4 Hz, 2H), 8.01 (s, 1H), 7.91 (d, *J* = 5.5 Hz, 1H), 7.83 (d, *J* = 3.8 Hz, 1H), 7.81–7.71 (m, 2H), 7.61–7.51 (m, 2H), 7.45 (d, *J* = 3.9 Hz, 1H), 7.27 (d, *J* = 6.0 Hz, 1H). ^{13}C NMR (151 MHz, DMSO-d$_6$) δ 186.99, 153.86, 152.46, 149.20, 145.21, 136.60, 132.94, 131.94, 131.49, 131.10, 128.71, 127.23, 127.04, 125.70, 125.62, 121.72, 118.80, 118.07, 115.28, 104.53. HRMS-APCI *m/z* calcd for $C_{22}H_{15}ClN_3O_4$ $[M+H]^+$, 420.0765, found 420.0746.

(*E*)-1-{4-[(7-Chloroquinolin-4-yl)amino]phenyl}-3-(2-nitrophenyl) prop-2-en-1-one (**2c**). Yellow powder; 32% yield; m.p.: 152–154°C; ^{1}H NMR (600 MHz, DMSO-d$_6$) δ 8.65 (d, *J* = 6.0 Hz, 1H), 8.55 (d, *J* = 9.0 Hz, 1H), 8.28 (d, *J* = 8.3 Hz, 2H), 8.10 (d, *J* = 8.2 Hz, 1H), 8.02–7.93 (m, 3H), 7.85 (t, *J* = 7.6 Hz, 1H), 7.77 (dd, *J* = 9.0, 2.2 Hz, 1H), 7.71 (t, *J* = 7.8 Hz, 1H), 7.59 (d, *J* = 8.3 Hz, 2H), 7.25 (s, 1H), 5.75 (s, 1H). ^{13}C NMR (151 MHz, DMSO-d$_6$) δ 187.89, 150.42, 149.32, 148.77, 144.67, 138.53, 136.91, 134.20, 133.55, 131.52, 131.16, 130.50, 130.25, 129.94, 127.18, 126.97, 125.77, 125.15, 124.31, 122.14, 118.53, 104.08. HRMS-APCI *m/z* calcd for $C_{24}H_{17}ClN_3O_3$ $[M+H]^+$, 430.0947, found 430.0953.

(*E*)-1-{4-[(7-Chloroquinolin-4-yl)amino]phenyl}-3-(3-nitrophenyl) prop-2-en-1-one (**2d**). Green powder; 62% yield; m.p.: 178–180°C; ^{1}H NMR (600 MHz, DMSO-d$_6$) δ 8.79 (t, *J* = 1.8 Hz, 1H), 8.65 (d, *J* = 6.1 Hz, 1H), 8.58 (d, *J* = 9.0 Hz, 1H), 8.36–8.32 (m, 3H), 8.27 (d, *J* = 0.7 Hz, 1H), 8.21 (d, *J* = 15.6 Hz, 1H), 8.02 (d, *J* = 2.0 Hz, 1H), 7.87 (d, *J* = 15.6 Hz, 1H), 7.81–7.74 (m, 2H), 7.61 (d, *J* = 8.4 Hz, 2H), 7.24 (d, *J* = 6.1 Hz, 1H). ^{13}C NMR (151 MHz, DMSO) δ 187.23, 148.29, 147.86, 141.01, 139.08, 138.31, 136.49, 134.96, 133.20, 132.67, 130.51, 130.22, 126.60, 125.17, 124.54, 124.48, 122.77, 121.62, 118.05, 117.72. HRMS-APCI *m/z* calcd for $C_{24}H_{17}ClN_3O_3$ $[M+H]^+$, 430.0954, found 430.0953.

(*E*)-1-{4-[(7-Chloroquinolin-4-yl)(4-methylbenzyl)aminophenyl}-3-(5-nitrofuran-2-yl)prop-2-en-1-one (**4a**). Brown powder; 45% yield; m.p.: 80–83°C; ^{1}H NMR (600 MHz, DMSO-d$_6$) δ 8.64 (dd, *J* = 11.4, 7.2 Hz, 1H), 8.43–8.34 (m, 1H), 8.24 (d, *J* = 8.3 Hz, 2H), 7.99–7.87 (m, 2H), 7.82 (dd, *J* = 10.6, 4.3 Hz, 1H), 7.72–7.56 (m, 2H), 7.53–7.40 (m, 3H), 7.19–6.87 (m, 4H), 6.74 (d, *J* = 51.2 Hz, 1H), 5.67 (s, 2H), 2.27 (s, 3H). ^{13}C NMR (151 MHz, DMSO-d$_6$) δ 187.30, 154.42, 153.84, 152.47, 148.21, 139.88, 138.00, 132.83, 131.52, 131.13, 131.04, 130.00, 128.81, 128.36, 128.28, 127.57, 127.16, 126.24, 125.65, 123.88, 118.11, 115.28, 108.83, 101.74, 56.33, 21.12. HRMS-APCI *m/z* calcd for $C_{30}H_{23}ClN_3O_4$ $[M+H]^+$, 524.1354, found 524.1372.

(*E*)-1-{4-[(7-Chloroquinolin-4-yl)(4-methylbenzylamino]phenyl}-3-(5-nitrothiophen-2-yl)prop-2-en-1-one (**4b**). Yellow powder; 8% yield; m.p.: 238–240°C; ^{1}H NMR (600 MHz, DMSO-d$_6$) δ 8.62 (d, *J* = 8.8 Hz, 1H), 8.37 (d, *J* = 27.6 Hz, 1H), 8.28 (d, *J* = 8.5 Hz, 2H), 8.17 (t, *J* = 5.5 Hz, 1H), 8.03 (d, *J* = 5.5 Hz, 1H), 7.95–7.88 (m, 2H), 7.81 (d, *J* = 4.4 Hz, 1H), 7.67 (d, *J* = 7.9 Hz, 1H), 7.41 (d, *J* = 6.8 Hz, 2H), 7.19 (s, 4H), 6.75–6.55 (m, 1H), 5.65 (s, 2H), 2.27 (s, 3H). ^{13}C NMR (151 MHz, DMSO-d$_6$) δ 186.83, 153.84, 151.53, 146.78, 139.37, 137.43, 134.37, 132.48, 130.97, 130.65, 130.58, 129.49, 127.12, 126.61, 125.53, 123.16, 117.33, 101.10, 56.01, 18.54.

(*E*)-1-{4-[(7-Chloroquinolin-4-yl)(4-methylbenzyl)amino]phenyl}-3-(3-nitrophenyl)prop-2-en-1-one (**4c**). Yellow powder; 14% yield; m.p.: 152–154°C; ^{1}H NMR (600 MHz, DMSO-d$_6$) δ 8.80 (dd, *J* = 6.7, 4.9 Hz, 1H), 8.62 (dd, *J* = 2.0, 7.0 Hz, 1H), 8.40–8.18 (m, 5H), 7.96–7.83 (m, 2H), 7.81–7.73 (m, 1H), 7.71–7.60 (m, 1H), 7.39 (s, 2H), 7.26–7.13 (m, 4H), 6.62 (d, *J* = 9.5 Hz, 1H), 5.63 (s, 2H), 2.28 (s, 3H). ^{13}C NMR (151 MHz, DMSO-d$_6$) δ 187.51, 153.82, 148.43, 141.02, 139.42, 137.38, 136.68, 135.08, 130.65, 130.36, 129.49, 127.15, 126.59, 124.78, 124.59, 122.94, 101.00, 55.06, 39.10, 20.65. HRMS-APCI *m/z* calcd for $C_{32}H_{25}ClN_3O_3$ $[M+H]^+$, 534.1553, found 534.1579.

(*E*)-1-{4-[(7-Chloroquinolin-4-yl)(4-methylbenzyl)amino]phenyl}-3-(2-nitrophenyl)prop-2-en-1-one (**4d**). Brown powder; 26% yield; m.p.: 141–144°C; ^{1}H NMR (600 MHz, DMSO-d_6) δ 8.70 (d, *J* = 8.9 Hz, 1H), 8.37–8.31 (m, 3H), 8.24 (dd, *J* = 7.9, 1.4 Hz, 1H), 8.12 (dd, *J* = 8.2, 1.3 Hz, 1H), 8.08–7.96 (m, 3H), 7.86 (td, *J* = 7.6, 1.3 Hz, 1H), 7.77 (s, 1H), 7.76–7.72 (m, 3H), 7.59–7.51 (m, 4H), 7.20 (s, 1H), 5.76 (s, 2H), 2.28 (s, 3H). ^{13}C NMR (151 MHz, DMSO-d_6) δ 188.14, 154.49, 149.31, 139.73, 138.79, 138.05, 134.25, 132.73, 131.57, 131.14, 130.23, 130.01, 129.99, 127.52, 127.18, 126.84, 125.20, 124.19, 101.88, 51.61, 21.14. HRMS-APCI *m/z* calcd for $C_{32}H_{25}CLN_3O_3$ $[M+H]^+$, 534.1570, found 534.1579.

(*E*)-1-{4-[(Benzyl)(7-chloroquinolin-4-yl)amino]phenyl}-3-(5-nitrothiophen-2-yl)prop-2-en-1-one (**4e**). Brown powder; 27% yield; m.p.: 295–297°C; ^{1}H NMR (600 MHz, DMSO-d_6) δ 8.88 (d, *J* = 7.4 Hz, 1H), 8.81 (d, *J* = 9.0 Hz, 1H), 8.64 (dd, *J* = 22.5, 7.7 Hz, 1H), 8.38 (d, *J* = 8.3 Hz, 2H), 8.34–8.24 (m, 2H), 8.19 (dd, *J* = 6.9, 4.3 Hz, 1H), 8.11–7.89 (m, 4H), 7.85 (d, *J* = 7.9 Hz, 1H), 7.74 (d, *J* = 8.2 Hz, 1H), 7.63 (d, *J* = 8.3 Hz, 1H), 7.43–7.20 (m, 3H), 5.98 (s, 2H). ^{13}C NMR (151 MHz, DMSO-d_6) δ 187.73, 147.02, 139.57, 135.48, 135.29, 131.71, 131.12, 131.05, 129.53, 128.88, 128.36, 127.25, 126.07, 125.97, 125.20, 123.42, 121.87, 118.96, 117.83, 110.19, 109.44, 107.99, 105.82, 102.50, 57.49.

(*E*)-1-{(4-[(4-Bromobenzyl)(7-chloroquinolin-4-yl)amino]phenyl}-3-(5-nitrofuran-2-yl)prop-2-en-1-one (**4f**). Orange powder; 22% yield; m.p.: 248–249°C; ^{1}H NMR (600 MHz, DMSO-d_6) δ 8.51 (d, *J* = 8.8 Hz, 1H), 8.17– 8.09 (m, 4H), 7.99 (d, *J* = 6.0 Hz, 1H), 7.92 (dd, *J* = 5.6, 13.0 Hz, 1H), 7.83 (dd, *J* = 4.0, 2.3 Hz, 1H), 7.68 (s, 1H), 7.64 (d, *J* = 2.1 Hz, 1H), 7.54–7.43 (m, 4H), 7.26–7.19 (m, 4H), 5.52 (s, 2H). ^{13}C NMR (151 MHz, DMSO-d_6) δ 186.95, 186.51, 154.08, 153.98, 152.40, 140.07, 136.06, 132.30, 131.15, 131.07, 129.21, 128.41, 127.94, 126.19, 125.76, 125.64, 125.27, 122.77, 121.48, 119.49, 117.88, 115.35, 101.21, 40.53.

(*E*)-1-{4-[(7-Chloroquinolin-4-yl)(4-(trifluoromethyl)benzyl)amino]phenyl}-3-(5-nitrofuran-2-yl)prop-2-en-1-one (**4g**). Brown powder; 35% yield; m.p.: 187–190°C; ^{1}H NMR (600 MHz, DMSO-d_6) δ 8.50 (d, *J* = 8.7 Hz, 1H), 8.18 (d, *J* = 8.2 Hz, 2H), 7.94 (d, *J* = 15.6 Hz, 2H), 7.83 (d, *J* = 3.9 Hz, 1H), 7.76 (d, *J* = 8.0 Hz, 2H), 7.61 (t, *J* = 13.7 Hz, 2H), 7.46 (t, *J* = 5.8 Hz, 4H), 7.18 (d, *J* = 8.0 Hz, 2H), 6.22 (s, 1H), 5.62 (s, 2H). ^{13}C NMR (151 MHz, DMSO-d_6) δ 186.91, 154.01, 152.39, 141.60, 140.19, 131.07, 128.74, 128.33, 128.03, 127.66, 126.29, 126.26, 125.80, 125.47, 123.67, 122.55, 117.81, 115.32, 101.22, 49.05. HRMS-APCI *m/z* calcd for $C_{30}H_{20}ClF_3N_3O_4$ $[M+H]^+$, 578.1083, found 578.1089.

(*E*)-1-{4-[(7-Chloroquinolin-4-yl)(4-(trifluoromethyl)benzyl)amino]phenyl}-3-(5-nitrothiophen-2-yl)prop-2-en-1-one (**4h**). Brown powder; 21% yield; m.p.: 238–240°C; ^{1}H NMR (600 MHz, DMSO-d_6) δ 8.68 (d, *J* = 9.0 Hz, 1H), 8.44 (d, *J* = 9.3 Hz, 1H), 8.32 (d, *J* = 8.2 Hz, 2H), 8.19 (d, *J* = 4.3 Hz, 1H), 8.04 (s, 1H), 7.93 (d, *J* = 15.4 Hz, 1H), 7.83 (d, *J* = 4.3 Hz, 1H), 7.77–7.69 (m, 4H), 7.49–7.45 (m, 4H), 7.40 (s, 1H), 5.88 (s, 2H). ^{13}C NMR (151 MHz, DMSO-d_6) δ 187.42, 154.54, 152.08, 147.23, 139.86, 135.01, 131.54, 131.17, 131.09, 128.98, 127.87, 127.68, 126.34, 126.31, 125.98, 40.43. HRMS-APCI *m/z* calcd for $C_{30}H_{20}ClF_3N_3O_3S$ $[M+H]^+$, 594.0832, found 594.0861.

(*E*)-1-{4-[(7-Chloroquinolin-4-yl)(4-(trifluoromethyl)benzyl)amino]phenyl}-3-(4-nitrophenyl)prop-2-en-1-one (**4i**). Yellow powder; 20% yield; m.p.: 160–162°C; ^{1}H NMR (600 MHz, DMSO-d_6) δ 8.73 (d, *J* = 8.8 Hz, 1H), 8.37 (d, *J* = 8.5 Hz, 2H), 8.32 (d, *J* = 8.5 Hz, 2H), 8.28–8.15 (m, 3H), 8.05 (s, 1H), 7.86–7.76 (m, 5H), 7.59–7.52 (m, 4H), 6.91 (s, 1H), 5.94 (s, 2H). ^{13}C NMR (151 MHz, DMSO-d_6) δ 188.17, 154.65, 148.62, 141.72, 141.42, 140.71, 139.87, 131.11, 130.33, 129.05, 127.90, 127.76, 126.60, 126.33, 126.31, 125.42, 124.42, 124.07, 123.62, 121.81, 117.82, 114.46, 102.90, 102.05, 102.05, 55.90. HRMS-APCI *m/z* calcd for $C_{32}H_{22}ClF_3N_3O_3$ $[M+H]^+$, 588.1273, found 588.1296.

4.1.4 | Synthesis of compounds 3a–3d

A round bottom flask was charged with 1.0 g (3.4 mmol) of intermediate **2**, 0.9 g (2 equivalents, 6.7 mmol) of potassium carbonate (K_2CO_3), 1.5 equivalents of appropriately substituted benzyl bromide, and 20 mL of *N*,*N*-dimethylformamide as a solvent. The mixture was heated under reflux and monitored by TLC for 24 h. After completion, the reaction mixture was cooled to room temperature and then washed with 20 mL of deionized water. The resulting residue afforded compound **3a**.

1-{4-[(7-Chloroquinolin-4-yl)(4-(trifluoromethyl)benzyl)amino]phenyl}ethan-1-one (**3d**). Yellow powder; 39% yield; m.p.: 219–220°C; ^{1}H NMR (600 MHz, DMSO-d_6) δ 8.41 (d, *J* = 8.6 Hz, 1H), 7.97–7.92 (m, 2H), 7.75 (d, *J* = 8.1 Hz, 2H), 7.68 (d, *J* = 8.0 Hz, 1H), 7.49–7.43 (m, 3H), 7.33 (dd, *J* = 8.7, 1.9 Hz, 1H), 6.99–6.94 (m, 2H), 5.93 (d, *J* = 7.9 Hz, 1H), 5.50 (s, 2H), 2.55 (s, 3H). ^{13}C NMR (151 MHz, DMSO-d_6) δ 196.89, 157.97, 153.70, 142.85, 141.97, 140.32, 136.67, 131.36, 130.47, 128.82, 128.61, 128.14, 127.59, 126.28, 126.25, 125.50, 124.31, 123.85, 123.70, 121.52, 116.12, 100.86, 54.13, 26.86. HRMS-APCI *m/z* calcd for $C_{25}H_{19}ClF_3N_2O$ $[M+H]^+$, 455.1130, found 455.1133.

4.2 | In vitro antiprotozoal evaluation

For the *L. infantum* assay, primary peritoneal mouse macrophages were infected with 4.5×10^5 parasites/well, and 3×10^4 macrophages were used as host cells. After 2 h of infection, serial dilutions of samples were added to the cells. The cells were then incubated for 5 days, after which the parasite burden was assessed microscopically by staining with a 10% Giemsa solution. The mean number of amastigotes (parasitic form) per macrophage was determined to evaluate the anti-*Leishmania* activity of the tested compounds.[39]

For the *T. cruzi* assay, the Tulahuen CL_2, β-galactosidase strain (which is sensitive to nifurtimox) was deployed, and MRC-5_{SV2} (human lung fibroblast) was used as host cells. The cells were infected with 4×10^4 parasites per well. Serial dilutions of the test samples were added 4 h after infection and incubated for 7 days at 37°C. After this, the substrate chlorophenolred β-D-galactopyranoside was added. Parasite burden was assessed by measuring spectrophotometrically

the change in color at 540 nm to determine the level of anti-*T. cruzi* activity of the tested compounds.[40]

The drug susceptibility of *T. brucei* Squib 427 and *T. b. rhodesiense* STIB-90050 was assessed using a resazurin assay. The parasites were cultured at a density of 1.5×10^4 parasites/well for *T. brucei* Squib 427 and 4×10^3 parasites/well for *T. b. rhodesiense*. Following incubation with varying concentrations of test samples, the parasites were further incubated for 72 h. Resazurin was then added, and the cells were incubated for an additional 24 h for *T. brucei* and 6 h for *T. b. rhodesiense*. Fluorescence detection was employed to measure the susceptibility of the parasites to the tested compounds.[41]

In each of the experiments, the growth of the parasites was compared to that of two control groups: the untreated but infected group (which showed 100% growth) and the noninfected group (which showed 0% growth). The results were expressed as the percentage reduction in parasite growth at different drug concentrations, and these values were then used to generate dose–response curves and calculate the EC_{50} values. We would like to emphasize that except for the inactive compounds, the results of this hit finding campaign are from three separate experiments showing high congruence of the EC_{50} values.

4.3 | In vitro cytotoxicity evaluation

To evaluate the cytotoxicity of compounds on MRC-5_{SV2} cells, the same methodology as described in a previous reference was followed. Briefly, 1.5×10^5 cells/mL were incubated with different concentrations of the test compounds at 37°C and 5% CO_2. Cell growth was compared to two control groups—untreated wells (which showed 100% cell growth) and medium-control wells (which showed 0% cell growth). After incubating for 3 days, cell viability was measured using a fluorescence-based assay involving the addition of 50 µL of resazurin per well, followed by measuring fluorescence (λ_{ex} 550 nm, λ_{em} 590 nm) after incubating for 4 h at 37°C. The results were expressed as a percentage reduction in cell growth or viability compared to the control wells, and an IC_{50} value was determined accordingly.[42]

ACKNOWLEDGMENTS

This project is funded by an MRC-SIR Grant awarded to RMB. The NMR spectra were recorded by Dr. Otto Daniel and Dr. Johan Jordaan of the SASOL Centre for Chemistry, North-West University. The authors are appreciative of the financial and infrastructural assistance rendered by North-West University, Potchefstroom campus. GC is a co-promotor of the 'Infla-Med' Centre of Excellence (www.uantwerpen.be/infla-med) and participates in COST Action CA21111.

CONFLICT OF INTEREST STATEMENT

The authors declare no conflicts of interest.

DATA AVAILABILITY STATEMENT

The data that supports the findings of this study are available in the Supporting Information Material of this article. The Supporting Information Material contains ^1H, ^{13}C NMR spectra, and HRMS spectra of compounds reported in this study.

ORCID

Carla B. Hartman http://orcid.org/0000-0001-8419-1446
Natascha Van Pelt http://orcid.org/0000-0001-8922-7903
An Matheeussen http://orcid.org/0000-0002-7507-1634
Richard M. Beteck http://orcid.org/0000-0002-6282-043X

REFERENCES

[1] D. Horn, *PLoS Negl. Trop. Dis.* **2022**, *16*, e0010040.
[2] R. Papagni, R. Novara, M. L. Minardi, L. Frallonardo, G. G. Panico, E. Pallara, S. Cotugno, T. Ascoli Bartoli, G. Guido, E. De Vita, A. Ricciardi, V. Totaro, M. Camporeale, F. V. Segala, D. F. Bavaro, G. Patti, G. Brindicci, C. Pellegrino, M. F. Mariani, G. Putoto, L. Sarmati, C. Castellani, A. Saracino, F. Di Gennaro, E. Nicastri, *Front. Trop. Dis.* **2023**, *4*, 1087003.
[3] R. Brun, J. Blum, F. Chappuis, C. Burri, *Lancet* **2010**, *375*, 148.
[4] T. T. Melachio Tanekou, C. U. Bouaka Tsakeng, I. Tirados, S. J. Torr, F. Njiokou, A. Acho, C. S. Wondji, *Med. Vet. Entomol.* **2022**, *36*, 260.
[5] M. M. G. Correia, J. V. M. Barboza, A. L. Espíndola, *Phys. A* **2021**, *582*, 126282.
[6] P. Büscher, G. Cecchi, V. Jamonneau, G. Priotto, *Lancet* **2017**, *390*, 2397.
[7] M. Berninger, I. Schmidt, A. Ponte-Sucre, U. Holzgrabe, *MedChemComm* **2017**, *8*, 1872.
[8] K. I. Kasozi, G. Zirintunda, F. Ssempijja, B. Buyinza, K. J. Alzahrani, K. Matama, H. N. Nakimbugwe, L. Alkazmi, D. Onanyang, P. Bogere, J. J. Ochieng, S. Islam, W. Matovu, D. P. Nalumenya, G. E. S. Batiha, L. O. Osuwat, M. Abdelhamid, T. Shen, L. Omadang, S. C. Welburn, *Front. Vet. Sci.* **2021**, *8*, 621699.
[9] L. J. Morrison, L. Vezza, T. Rowan, J. C. Hope, *Trends Parasitol.* **2016**, *32*, 599.
[10] H. Holt, R. Selby, C. Mumba, G. Napier, J. Guitian, *Parasit. Vectors* **2016**, *9*, 53.
[11] J. Clayton, *Nature* **2010**, *465*, S4.
[12] World Health Organization, https://www.who.int/publications/i/item/9789240010352 (accessed: July 2023).
[13] S. Sundar, J. Chakravarty, L. P. Meena, *Expert Opin. Orphan Drugs* **2019**, *7*, 1.
[14] S. Singh, R. Sivakumar, *J. Infect. Chemother.* **2004**, *10*, 307.
[15] M. De Rycker, S. Wyllie, D. Horn, K. D. Read, I. H. Gilbert, *Nat. Rev. Microbiol.* **2023**, *21*, 35.
[16] R. Kaur, K. Kumar, *Eur. J. Med. Chem.* **2021**, *215*, 113220.
[17] N. A. Harry, S. M. Ujwaldev, G. Anilkumar, *Org. Biomol. Chem.* **2020**, *18*, 9775.
[18] F. R. B. Bokosi, R. M. Beteck, D. Laming, H. C. Hoppe, T. Tshiwawa, S. D. Khanye, *Arch. Pharm.* **2021**, *354*, e2000331.
[19] A. S. G. Nefertiti, M. M. Batista, P. B. Da Silva, D. G. J. Batista, C. F. Da Silva, R. B. Peres, E. C. Torres-Santos, E. F. Cunha-Junior, E. Holt, D. W. Boykin, R. Brun, T. Wenzler, M. Soeiro, *Antimicrob. Agents Chemother.* **2018**, *62*, e01936.
[20] M. Yousuf, D. Mukherjee, S. Dey, C. Pal, S. Adhikari, *Eur. J. Med. Chem.* **2016**, *124*, 468.
[21] F. R. B. Bokosi, R. M. Beteck, A. Jordaan, R. Seldon, D. F. Warner, T. Tshiwawa, K. Lobb, S. D. Khanye, *J. Heterocycl. Chem.* **2021**, *58*, 2140.
[22] N. Sun, R. L. Du, Y. Y. Zheng, B. H. Huang, Q. Guo, R. F. Zhang, K. Y. Wong, Y. J. Lu, *Eur. J. Med. Chem.* **2017**, *135*, 1.
[23] J. E. Charris, M. C. Monasterios, M. E. Acosta, M. A. Rodríguez, N. D. Gamboa, G. P. Martínez, H. R. Rojas, M. R. Mijares, J. B. De Sanctis, *Med. Chem. Res.* **2019**, *28*, 2050.
[24] R. M. Beteck, L. J. Legoabe, M. Isaacs, S. D. Khanye, D. Laming, H. C. Hoppe, *Medicina* **2019**, *55*, 206.

[25] D. Elkhalifa, I. Al-Hashimi, A.-E. Al Moustafa, A. Khalil, *J. Drug Targeting* **2021**, *29*, 403.
[26] K. T. Angula, L. J. Legoabe, T. Swart, H. C. Hoppe, R. M. Beteck, *Eur. J. Med. Chem.* **2022**, *227*, 113913.
[27] T. Constantinescu, C. N. Lungu, *Int. J. Mol. Sci.* **2021**, *22*, 11306.
[28] M. Roussaki, B. Hall, S. C. Lima, A. C. da Silva, S. Wilkinson, A. Detsi, *Bioorg. Med. Chem. Lett.* **2023**, *23*, 6436.
[29] Z. Qiao, Q. Wang, F. Zhang, Z. Wang, T. Bowling, B. Nare, R. T. Jacobs, J. Zhang, D. Ding, Y. Liu, H. Zhou, *J. Med. Chem.* **2012**, *55*, 3553.
[30] S. F. Nielsen, M. Larsen, T. Boesen, K. Schønning, H. Kromann, *J. Med. Chem.* **2005**, *48*, 2667.
[31] P. S. Dube, L. J. Legoabe, A. Jordaan, O. J. Jesumoroti, T. Tshiwawa, D. F. Warner, R. M. Beteck, *Eur. J. Med. Chem.* **2021**, *213*, 113207.
[32] C. du Preez, L. J. Legoabe, A. Jordaan, O. J. Jesumoroti, D. F. Warner, R. M. Beteck, *Chem. Biol. Drug Des.* **2023**, *101*, 717.
[33] D. Hart, L. J. Legoabe, O. J. Jesumoroti, A. Jordaan, D. F. Warner, R. Steventon, R. M. Beteck, *Chem. Biodivers.* **2022**, *19*, e202200729.
[34] K. Nepali, H. Y., Lee, J. P., Liou, *J. Med. Chem.* **2019**, *62*, 2851.
[35] J. G. Hurdle, R. B. Lee, N. R. Budha, E. I. Carson, J. Qi, M. S. Scherman, S. H. Cho, M. R. McNeil, A. J. Lenaerts, S. G. Franzblau, B. Meibohm, R. E. Lee, *J. Antimicrob. Chemother.* **2008**, *62*, 1037.
[36] A. S. Ressurreição, D. Gonçalves, A. R. Sitoe, I. S. Albuquerque, J. Gut, A. Góis, L. M. Gonçalves, M. R. Bronze, T. Hanscheid, G. A. Biagini, P. J. Rosenthal, M. Prudêncio, P. O'Neill, M. M. Mota, F. Lopes, R. Moreira, *J. Med. Chem.* **2013**, *56*, 7679.
[37] R. M. Beteck, M. Isaacs, L. J. Legoabe, H. C. Hoppe, C. C. Tam, J. H. Kim, J. P. Petzer, L. W. Cheng, Q. Quiambao, K. M. Land, S. D. Khanye, *Arch. Pharm.* **2023**, *356*, e2200409.
[38] M. Sharma, V. Chaturvedi, Y. K. Manju, S. Bhatnagar, K. Srivastava, S. K. Puri, P. M. S. Chauhan, *Eur. J. Med. Chem.* **2009**, *44*, 2081.
[39] K. J. Setshedi, R. M. Beteck, O. J. Jesumoroti, K. Ilbeigi, D. Mabille, G. Caljon, F. Van der Kooy, L. J. Legoabe, *Chem. Biol. Drug Des.* **2023**, *102*, 763.
[40] J. Bouton, L. Ferreira de Almeida Fiuza, C. Cardoso Santos, M. A. Mazzarella, M. N. C. Soeiro, L. Maes, I. Karalic, G. Caljon, S. Van Calenbergh, *J. Med. Chem.* **2021**, *64*, 4206.
[41] F. Hulpia, D. Mabille, G. D. Campagnaro, G. Schumann, L. Maes, I. Roditi, A. Hofer, H. P. de Koning, G. Caljon, S. Van Calenbergh, *Nat. Commun.* **2019**, *10*, 5564.
[42] D. Mabille, K. Ilbeigi, S. Hendrickx, M. A. Ungogo, F. Hulpia, C. Lin, L. Maes, H. P. de Koning, S. Van Calenbergh, G. Caljon, *Int. J. Parasitol.: Drugs Drug Resist.* **2022**, *19*, 21.

SUPPORTING INFORMATION

Additional supporting information can be found online in the Supporting Information section at the end of this article.

How to cite this article: C. B. Hartman, P. S. Dube, L. J. Legoabe, N. Van Pelt, A. Matheeussen, G. Caljon, R. M. Beteck, *Arch. Pharm.* **2024**, e2300319.
https://doi.org/10.1002/ardp.202300319